

Fluorescent hydrogels formed by CH– π and π – π interactions as the main driving forces: an approach toward understanding the relationship between fluorescence and structure†

Cite this: DOI: 10.1039/c2cc37249e

Received 4th October 2012,
Accepted 2nd January 2013

DOI: 10.1039/c2cc37249e

www.rsc.org/chemcomm

Jinho Ahn, Sunhong Park, Ji Ha Lee, Sung Ho Jung, Seung-Jin Moon and Jong Hwa Jung*

Amide-linked tripyridine derivatives 1, with a *para*-substituent, and 2, with a *meta*-substituent, were gelled in water or water–DMSO. The gelation capabilities of 1 and 2 were attributed to the cooperative effects of mainly CH– π and π – π stacking or strong intermolecular hydrogen bonding interactions between the amide groups. The fluorescence properties of gels 1 and 2 were dependent on the binding strength of the π – π stacking.

Low molecular mass gelators (LMMGs) have drawn widespread attention from both theoretical and practical points of view.^{1,2} These small organic compounds can efficiently encapsulate various solvents through the formation of three-dimensional networks made up of fibrous aggregates.^{3–7} To form a gel with a given solvent, elegant molecular design is necessary to maintain the balance between crystallization and solubility of the LMMGs. LMMGs gelate based on their π – π stacking, van der Waals, intermolecular hydrogen bonding and solvophobic properties.

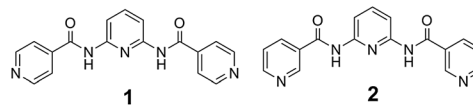
With respect to the molecular design of LMMGs, the relationship between the molecular packing of the gelators in their bulk crystal state and their less well ordered aggregates within the gels remains poorly understood.⁸ A better understanding of molecular packing may help not only tune the supramolecular structures of LMMGs in a gel by tailoring their intermolecular interactions but may also prevent the collapse of the gels formed by LMMGs, which is a disadvantage of this kind of material as compared to polymer gels. The molecular packing of LMMGs in self-assembled gels has been examined by IR, NMR spectroscopy, X-ray diffraction and scattering techniques. However, these methods give limited or indirect information about the molecular packing structures because of the complicated and hierarchical structures of the wet gel.² In contrast, single crystal X-ray crystallography provides the most precise and complete information about molecular packing in the solid phase.^{9,10} However, studying

the molecular packing in gel chemistry by single crystal X-ray crystallography gives rise to two problems. First, a single crystal of a gelator suitable for X-ray diffraction experiments is difficult to obtain because these molecules aggregate to form gel fibers or needles instead of large crystals. Second, differences in molecular packing between single crystals and gels are difficult to distinguish because gels and crystals arise from distinctly different conditions. Therefore, few systematic investigations of the influence of molecular packing on molecular gelling ability have been reported. For example, the Menger¹¹ and Shinkai¹² groups have successfully reported the molecular orientation or the driving force for gel formation. In contrast, no study has yet reported the relationship between the physical properties and the molecular packing structures of gelators, which is very important for applications of these compounds. In particular, numerous reports have used IR studies to define the intermolecular hydrogen bonding interactions of the amide groups of gelators as the main driving force in gel formation.^{13,14} However, it is still not clear whether the amide groups of gelators form intermolecular hydrogen bonding interactions.

Herein, we examine the relationship between the molecular structures of pyridine-based hydrogelators and the stabilities of the gels. Our results demonstrate the importance of intermolecular hydrogen bonding interactions. We show that interactions such as those between the N atom of pyridine and –NH, the –C=O and –CH of pyridine, and π – π and CH– π interactions are the main forces that drive gel formation. In particular, the binding strengths of π – π and CH– π interactions in the gel states have a great influence on the fluorescence properties. A combinatorial analysis of the X-ray data of both single crystals and xerogels, fluorescence spectra and FT IR spectra of both crystals and xerogels demonstrated that the tripyridine structures 1 and 2 formed three dimensional structures in the gel state. The number of intermolecular hydrogen bonds and

Department of Chemistry and Research Institute of Natural Science, Gyeongsang National University, Jinju 660-701, Korea. E-mail: jonghwa@gnu.ac.kr

† Electronic supplementary information (ESI) available: Experimental details, SEM images, AFM images, XRD patterns, rheometer measurement. CCDC 676429 and 905197. For ESI and crystallographic data in CIF or other electronic format see DOI: 10.1039/c2cc37249e



π - π interactions in gel formation are also strongly dependent on the mechanical stress.

The pyridine-based gelators **1** and **2** were synthesized by a previously reported method.¹⁵ They consisted of three pyridine groups, but with different substituents. The structures were identified by ¹H NMR, FT IR, mass spectroscopy and elemental analyses (see ESI†).

Twenty solvents were employed to evaluate the gelling abilities of **1** and **2**. The results are summarized in Table S1 (ESI†). It was evident that **1** and **2** were soluble in the four polar solvents methanol, dimethyl formamide (DMF), tetrahydrofuran (THF) and 1,4-dioxane, but were insoluble in the three non-polar solvents, tetrachloromethane, cyclohexane and toluene. Interestingly, *para*-substituted **1** can gelate in water under neutral, basic and weakly acidic conditions (Fig. S1, ESI†). On the other hand, the *meta*-substituted **2** can gelate in water–DMSO (1 : 1 v/v) at all pH values (Fig. S2, ESI†). These results would be related to the pK_b values of the pyridine derivatives. The pK_b (ca. 4.6) of the pyridyl carboxyl acid bearing the *para*-substituent is much higher than that of the pyridyl carboxylic acid with a *meta*-substituent (ca. 7.29).¹⁶ Therefore, the *para*-substituted **1** was protonated under acidic conditions, making it soluble in water. On the other hand, the *meta*-substituted **2** was not protonated under acidic conditions, making it insoluble in pure water. The gelation of the *para*-substituted **1** is due to environmental influences under specific solvent conditions.

To gain insights into the aggregation morphologies of the hydrogels **1** and **2** at different pH values, samples of dried gels **1** and **2** prepared at pH values ranging from 2–13 were transferred onto a glass slide and subjected to scanning electron microscopy (SEM) and atomic force microscopy (AFM) observations. Micrographs of hydrogel **1** obtained at pH 7 showed entangled three-dimensional networks of bundles of fiber aggregates (Fig. 1a and Fig. S3, ESI†), whereas the hydrogel **1** obtained at pH 12 showed a linear fiber structure with widths of 500–700 nm (Fig. S4, ESI†). The hydrogels **2** prepared at pH 7 and 12 were also entangled three-dimensional networks of fibers with narrower widths ranging from 40–60 nm and lengths from 10–40 nm (Fig. 1b; Fig. S5b and S6, ESI†) whereas the image of hydrogel **2** at pH 2 revealed a thicker rod-like fiber structure of 0.5–1.6 μ m in length and 20–40 nm in width (Fig. S5a, ESI†).

To compare the fluorescence properties of gels **1** and **2**, we recorded the fluorescence spectra of hydrogels **1** and **2** at pH 7 (Fig. 2). Upon excitation at 330 nm, the *para*-substituted gel **1** emitted blue fluorescence at 427 nm. The fluorescent emission intensity of gel **1** was relatively higher than that of the *meta*-substituted gel **2** under the same conditions. The relatively weak emission of the *meta*-substituted gel **2** is attributed to the relatively

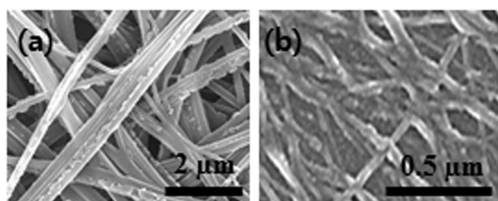


Fig. 1 SEM images of hydrogels (a) **1** and (b) **2** prepared from water and water–DMSO (1 : 1 v/v) at pH 7, respectively.

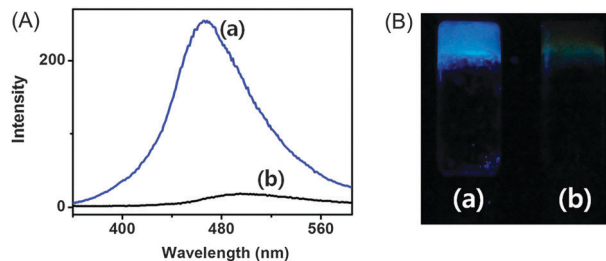


Fig. 2 (A) The fluorescence spectra and (B) photograph of hydrogels (a) **1** (3.0 wt%) and (b) **2** (3.0 wt%) at pH 7 under UV light.

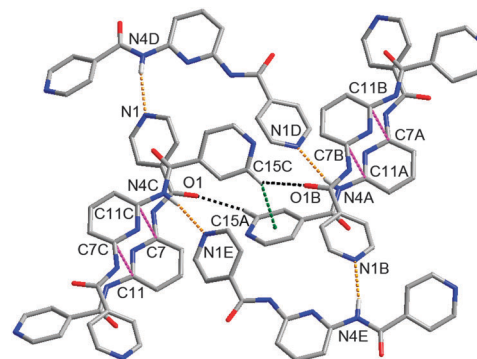


Fig. 3 Packing structure of **1** sustained by N–H...N (yellow dashed lines), C–H...O (black dashed lines), π ... π (pink dashed lines) and C–H... π (green dashed lines) bonds. Symmetry codes for **1**: A: $x, -1 + y, z$; B: $0.5 - x, -1 - y, -0.5 + z$; C: $0.5 - x, -y, -0.5 + z$; D: $-x, -0.5 + y, 1.5 - z$; E: $0.5 + x, -0.5 - y, 1 - z$.

greater quenching effect induced by the *meta* substitution pattern than that occurring in the *para*-substituted gel **1**. This observation is in good agreement with our analysis of their packing structure.

To further elucidate the driving forces for gel formation and the mechanism of fluorescence of hydrogels **1** and **2** obtained at pH 7, we prepared single crystals, yellow in color, suitable for X-ray analysis from solutions of **1** and **2** at pH 7 (Fig. 3 and 4). Detailed crystallographic data are summarized in Table S2 (ESI†). Compound **1** in neutral form (grown at pH 7) is alternately arranged along the *b* axis to form a herringbone-type array.¹⁵ The molecular conformation and

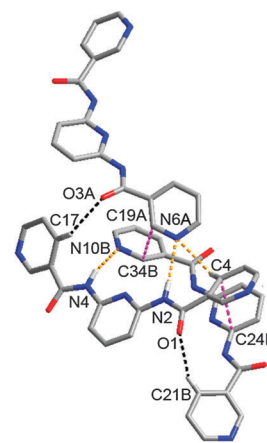


Fig. 4 Packing structure of **2** sustained by N–H...N (yellow dashed lines), C–H...O (black dashed lines) and π ... π (pink dashed lines) bonds. Symmetry codes for **2**: A: $1 - x, 1 - y, 1 - z$; B: $1 - x, 0.5 + y, 0.5 - z$; C: $x, 0.5 - y, 0.5 + z$.

the array are stabilized by formation of several intermolecular hydrogen bonds such as C–H···O, C–H···N(pyridine) and N–H(amide)···N(pyridine) types, which have bond lengths of *ca.* 2.3–2.6 Å (Fig. S7C and Table S3, ESI†). Intermolecular hydrogen bonds between an amide NH and CO were not observed. Instead, an offset face-to-face type of weak π – π stacking and CH··· π interactions between pyridine moieties in neighboring arrays were observed with the shortest distance between two carbon atoms in each aromatic ring being 3.4 and 3.5 Å, and edge-to-centroid distance 2.6 Å (Fig. S7D, ESI†).

meta-Substituted **2** is also formed by two different intermolecular hydrogen bonding interactions. The crystal structure of **2** is stabilized primarily by the formation of intermolecular hydrogen bonds between a hydrogen of pyridine and an amide, and the –C=O and –CH of the pyridine. These hydrogen bonds have bond lengths of *ca.* 2.2–2.8 Å (Fig. S8C and Table S4, ESI†). The offset face-to-face type π – π stacking between pyridine moieties in neighboring arrays was also observed with the shortest distance between two carbon atoms in each aromatic ring being 3.2 and 3.3 Å (Fig. S8D, ESI†), which is relatively stronger than the interactions obtained for *para*-substituted **1**. In particular, the intermolecular H-bonds between –C=O and –NH in *meta*-substituted **2** have a bond length of 2.26 Å. The relatively strong π – π stacking interaction in **2** induced the larger quenching effect.¹⁷

Wide-angle X-ray diffraction (WAXD) was used to probe the molecular packing of **1** in either the xerogel or the bulk crystal. Powder XRD patterns of xerogels **1** and **2** prepared under neutral conditions had the same diffraction pattern as that of the bulk crystal prepared from water or methanol. Furthermore, the strong similarities between the powder XRD patterns of **1** and **2** in the bulk crystal and those of the xerogels **1** and **2** suggested that the molecular packing of **1** and **2** in the bulk crystal was the same as the molecular packing of gelators in the gel state (Fig. S9, ESI†). The results also suggest the view that the large quenching effect of the gel **2** is due to relatively strong π – π stacking between the pyridine groups.

Rheological information is an indicator of the behavior of the gels when they are exposed to mechanical stress. The “storage” (or “elastic”) modulus G' represents the ability of the deformed material to “snap back” to its original geometry, and the “loss” (or “viscous”) modulus G'' represents the tendency of a material to flow under stress. Two rheological criteria required for a gel are: (i) the independence of the dynamic elastic modulus, G' , with respect to the oscillatory frequency, and (ii) G' must exceed the loss modulus G'' by about 1 order of magnitude.

We first used dynamic strain sweep to determine the proper conditions for the dynamic frequency sweep of the gels **1** and **2** at the same concentration. As shown in Fig. S10A (ESI†), the values of the storage modulus (G') and the loss modulus (G'') exhibited a weak dependence from 0.1 to 1.0% of strain (with G' dominating G''), indicating that the sample is a gel. The values of both G' and G'' of the gel **1** were *ca.* 100-fold higher than that of gel **2**, because the strength of gel **1** is greater than that of the gel **2**. These results reflect the stabilization of gel **1** by two H-bonding and one –CH– π stacking interactions.

We used dynamic frequency sweep to study the gel after setting the strain amplitude at 0.8% (within the linear response region of the strain amplitude). G' and G'' were almost constant with the increase of frequency from 0.1 to 100 rad s^{–1} (Fig. S10B, ESI†).

The value of G' was about 3 times larger than that of G'' over the whole range (0.1–100 rad s^{–1}), suggesting that the gel is fairly tolerant to external force. As observed by changes of dynamic strain sweep, the values of both G' and G'' of the gel **1** were also 100-times larger than that of the gel **2**. Furthermore, time-dependent oscillation measurements were used to monitor the gelation processes of gels **1** and **2** (Fig. S10C, ESI†). The time sweep shows the rapid increase of G' and G'' in the initial stage of gelation, followed by a slower long term approach to a final pseudo-equilibrium plateau. At the end of the experiment, the value of G' was about an order of magnitude higher than G'' .

In conclusion, our comparisons of the crystal and gel structures of **1** and **2** have provided complete information about their molecular packing. The XRD patterns of both the crystals and the gels indicated the same crystal structure. Clearly, π – π stacking and hydrogen bonding are crucial factors in the assembly of small-molecular gelators. The gelation abilities of pyridine-based derivatives **1** and **2** are strongly dependent on the p*K*_b values. More interestingly, the fluorescence intensity of *meta*-substituted **2** was relatively smaller than that of the *para*-substituted **1**, indicating that the emission property is also dependent on the binding strength of the π – π stacking. As a complementary armory of dynamic oscillation, steady shear experiments indicated that the gel formed for the *para*-substituted gel **1** is relatively strong and is a thermally resistant network as compared to the gel **2** bearing the *meta*-substituent. The fluorescence property of the pyridine-based gels may be suitable for applications in optoelectronic devices.

This work was supported by a grant from World Class Project (WCU: R32-2008-000-20003-0) and NRF (2012R1A4A1027750 and 2012-002547) supported by Ministry of Education Science and Technology, Korea. In addition, this work was partially supported by a grant from the Next-Generation BioGreen 21 Program (SSAC, grant#: PJ009041022012), Rural development Administration, Korea.

Notes and references

- P. Terech and R. G. Weiss, *Chem. Rev.*, 1997, **97**, 3133.
- L. A. Estroff and A. D. Hamilton, *Chem. Rev.*, 2004, **104**, 1201.
- J. H. van Esch and B. L. Feringa, *Angew. Chem., Int. Ed.*, 2000, **39**, 2263.
- J. Becerril, M. I. Burguete, E. B. scuder, S. V. Luis, J. F. Miravet and M. Querol, *Chem. Commun.*, 2002, 738.
- K. Yoza, Y. Ono, K. Yoshihara, T. Akao, H. Shinmori, M. Takeuchi, S. Shinkai and D. N. Reinhoudt, *Chem. Commun.*, 1998, 907.
- R. J. H. Hafkamp, B. P. A. Kokke, I. M. Danke, H. P. M. Geurts, A. E. Rowan, M. C. Feiters and R. J. M. Nolte, *Chem. Commun.*, 1997, 545.
- I. Furman and R. G. Weiss, *Langmuir*, 1993, **9**, 2084.
- K. A. Houton, K. L. Morris, L. Chen, M. Schmidtman, J. T. A. Jones, L. C. Serpell, G. O. Lloyd and D. J. Adams, *Langmuir*, 2012, **28**, 9797.
- J. Cui, Z. Shen and X. Wan, *Langmuir*, 2010, **26**, 97.
- W. Boomgaarden, F. Vögtle, M. Nieger and H. Hupfer, *Chem.–Eur. J.*, 1999, **5**, 345.
- F. M. Menger and K. L. Caran, *J. Am. Chem. Soc.*, 2000, **122**, 11679.
- O. Gronwald and S. Shinkai, *Chem.–Eur. J.*, 2001, **7**, 4329.
- M. M. Piepenbrock, G. O. Lloyd, N. Clarke and J. W. Steed, *Chem. Rev.*, 2010, **110**, 1960.
- M. Llusar and C. Sanchez, *Chem. Mater.*, 2008, **20**, 782.
- T. H. Kim, J. Seo, S. J. Lee, S. S. Lee, J. Kim and J. H. Jung, *Chem. Mater.*, 2007, **19**, 5815.
- T. W. G. Solomons and C. B. Fryhle, *Organic Chemistry*, John Wiley & Sons (Asia), Hoboken, 2008.
- Z. Q. Liang, Y. Z. Li, J. X. Yang, Y. Ren and X. T. Tao, *Tetrahedron Lett.*, 2011, **52**, 1329.